Acta Cryst C STRUCTURAL CHEMISTRY
ISSN 2053-2296

Crystal structure and photoluminescence properties of a new monomeric copper(II) complex: bis(3-{[(3-hydroxypropyl)imino]methyl}-4-nitrophenolato-κ^3O,N,O')copper(II)

Cagdas Kocak,[a] Gorkem Oylumluoglu,[a]* Adem Donmez,[a] M. Burak Coban,[b,c] Ugur Erkarslan,[a] Muhittin Aygun[d] and Hulya Kara[a,b]

[a]Department of Physics, Molecular Nano-Materials Laboratory, Mugla Sitki Kocman University, Mugla, Turkey, [b]Department of Physics, Balikesir University, Balikesir, Turkey, [c]Science and Technology Application and Research Center (BUBTAM), Balikesir University, Balikesir, Turkey, and [d]Department of Physics, 9 Eylul University, Izmir, Turkey. *Correspondence e-mail: gorkem@mu.edu.tr

Received 18 February 2017
Accepted 20 April 2017

Edited by T.-B. Lu, Sun Yat-Sen University, People's Republic of China

Keywords: monomeric copper(II) complex; photoluminescence; phenolate; crystal structure; hydrogen bonding.

CCDC reference: 1533191

Supporting information: this article has supporting information at journals.iucr.org/c

Copper(II)–Schiff base complexes have attracted extensive interest due to their structural, electronic, magnetic and luminescence properties. The title novel monomeric Cu^{II} complex, $[Cu(C_{10}H_{11}N_2O_4)_2]$, has been synthesized by the reaction of 3-{[(3-hydroxypropyl)imino]methyl}-4-nitrophenol (H_2L) and copper(II) acetate monohydrate in methanol, and was characterized by elemental analysis, UV and IR spectroscopies, single-crystal X-ray diffraction analysis and a photoluminescence study. The Cu^{II} atom is located on a centre of inversion and is coordinated by two imine N atoms, two phenoxy O atoms in a mutual *trans* disposition and two hydroxy O atoms in axial positions, forming an elongated octahedral geometry. In the crystal, intermolecular O—H···O hydrogen bonds link the molecules to form a one-dimensional chain structure and π–π contacts also connect the molecules to form a three-dimensional structure. The solid-state photoluminescence properties of the complex and free H_2L have been investigated at room temperature in the visible region. When the complex and H_2L are excited under UV light at 349 nm, the complex displays a strong green emission at 520 nm and H_2L displays a blue emission at 480 nm.

1. Introduction

Transition-metal compounds have been of great interest and importance for researchers since they play a critical role in the development of coordination chemistry in structures such as one-dimensional chains, two-dimensional layers, three-dimensional frameworks and especially metal–organic frameworks (MOFs) (Paul *et al.*, 2016; Pal *et al.*, 2016; Kongchoo *et al.*, 2016). They have great potential applications, for example, as luminescent probes, in catalysis (Gungor *et al.*, 2014), as sensors (Zheng *et al.*, 2016), in nonlinear optics (Karakas *et al.*, 2006), as single-molecule magnets (SMMs) (Kahn, 1993; Caneschi *et al.*, 2015; Gungor *et al.*, 2015; Blacque *et al.*, 2016) and for exhibiting biological activities (Jamaludin *et al.*, 2016), and also in solar-cell and photovoltaic technologies (Freitag *et al.*, 2016; Magni *et al.*, 2016).

Moreover, luminescent compounds have attracted attention because of their applications, particularly in modern electronics, as materials for producing organic light emitting diodes (OLEDs) (Sasabe & Kido, 2011; Petrova & Tomova, 2009; Kelley *et al.*, 2004). In this context, Schiff base ligands have been used as fluorescent sensors for the detection of certain metal ions (Zhou *et al.*, 2010). Cu^{II}–Schiff base complexes have also attracted extensive interest due to their structural,

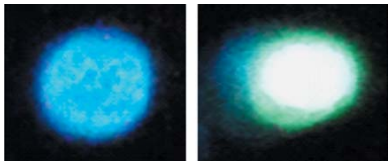

Table 1
Experimental details.

Crystal data	
Chemical formula	$[Cu(C_{10}H_{11}N_2O_4)_2]$
M_r	509.95
Crystal system, space group	Monoclinic, $P2_1/c$
Temperature (K)	292
a, b, c (Å)	10.5788 (11), 6.2806 (5), 15.8478 (19)
β (°)	105.272 (12)
V (Å^3)	1015.76 (19)
Z	2
Radiation type	Mo $K\alpha$
μ (mm^{-1})	1.14
Crystal size (mm)	0.25 × 0.15 × 0.06
Data collection	
Diffractometer	Rigaku OD Xcalibur Eos
Absorption correction	Analytical [*CrysAlis PRO* (Rigaku OD, 2015), based on expressions derived by Clark & Reid (1995)]
T_{min}, T_{max}	0.823, 0.947
No. of measured, independent and observed [$I > 2\sigma(I)$] reflections	3722, 1908, 1303
R_{int}	0.046
(sin $\theta/\lambda)_{max}$ (Å^{-1})	0.610
Refinement	
$R[F^2 > 2\sigma(F^2)]$, $wR(F^2)$, S	0.056, 0.120, 1.03
No. of reflections	1908
No. of parameters	152
H-atom treatment	H-atom parameters constrained
$\Delta\rho_{max}$, $\Delta\rho_{min}$ (e Å^{-3})	0.46, −0.44

Computer programs: *CrysAlis PRO* (Rigaku OD, 2015), *SHELXT* (Sheldrick, 2015*a*), *SHELXL2016* (Sheldrick, 2015*b*) and *OLEX2* (Dolomanov *et al.*, 2009).

electronic, magnetic and luminescence properties (Yahsi, 2016; Yashi *et al.*, 2016; Chang *et al.*, 2006; Keypour *et al.*, 2016; Safaei *et al.*, 2011; Hopa & Cokay, 2016*a*; Erkarslan *et al.*, 2016; Naskar *et al.*, 2010; Obali & Ucan, 2015).

Recently, our research group and others have reported the synthesis and structural characterization of Cu^{II} complexes containing ONNO-, ONO- and NNO-type Schiff base ligands (Gungor & Kara, 2012; Yahsi & Kara, 2013; Keypour *et al.*, 2015, Gungor, 2017). Since copper(II) quenches luminescence, examples of copper(I,II) and copper(II) luminescent complexes are scarce (Li *et al.*, 2009; Delgado *et al.*, 2010; Wu *et al.*, 2010). In this context, and in view of the importance of Cu^{II} complexes and in an effort to enlarge the library of such complexes, we report here the synthesis of a new Cu^{II} complex, namely bis(3-{[(3-hydroxypropyl)imino]methyl}-4-nitrophenolato-κ^3O,N,O')copper(II), (1), along with its characterization, single-crystal X-ray structure, UV and IR spectroscopic analyses and photoluminescence study.

2. Experimental

All chemicals and solvents used for the synthesis of (1) were of reagent grade and were used without further purification. Elemental (C, H and N) analyses were carried out using standard methods. FT–IR spectra were measured with a PerkinElmer Spectrum 65 instrument in the range 4000–600 cm^{-1}. Solid-state luminescence spectra in the visible region were measured at room temperature with an ANDOR SR500i-BL Photoluminescence Spectrometer equipped with a triple grating and with an air-cooled CCD camera as detector. The measurements were carried out using the excitation source (349 nm) of a Spectra-physics Nd:YLF laser with a 5 ns pulse width and 1.3 mJ of energy per pulse as the source.

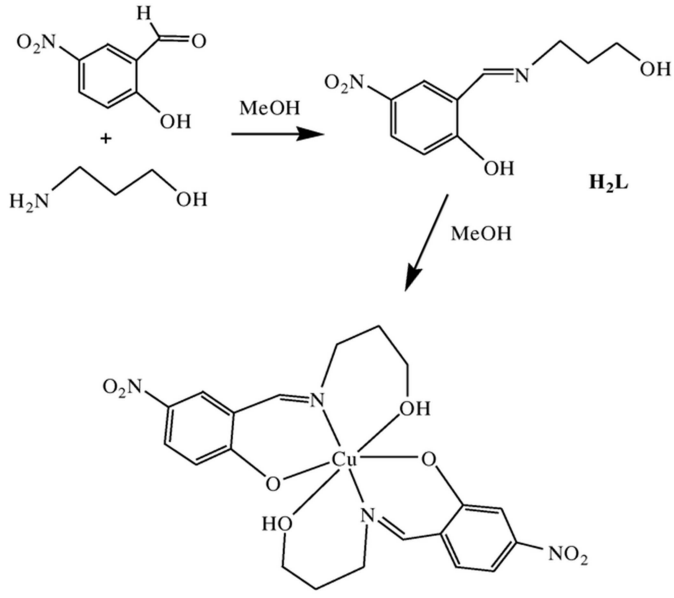

Scheme 1

2.1. Synthesis of Schiff base H_2L and complex (1)

3-{[(3-Hydroxypropyl)imino]methyl}-4-nitrophenol (H_2L) was prepared by mixing 5-nitrosalicylaldehyde (1 mmol) and 3-aminopropan-1-ol (1 mmol) in a 1:1 molar ratio in hot methanol (50 ml) according to the literature methods of Gungor *et al.* (2012) and Celen *et al.* (2013). Yellow crystals were obtained (yield 85%). Analysis calculated for $C_{10}H_{12}N_2O_4$: C 53.57, H 5.39, N 12.49%; found: C 53.59, H 5.38, N 12.48%.

The solution obtained was stirred at 338 K for 30 min and the yellow product precipitated from the solution on cooling. Complex (1) was prepared by addition of copper(II) acetate

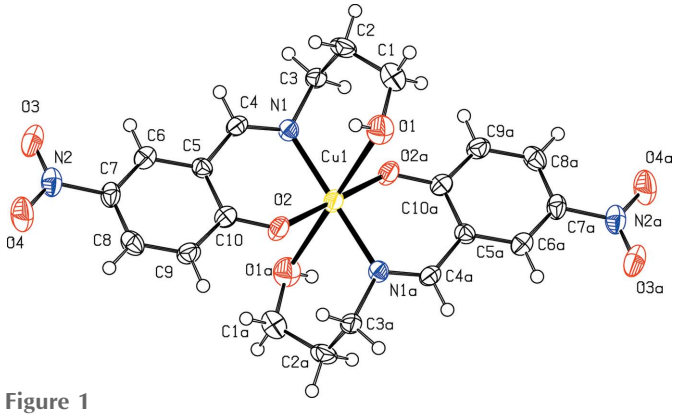

Figure 1
The molecular structure of complex (1), showing the atom-labelling scheme and 50% probability displacement ellipsoids. [Symmetry code: (i) $-x, -y + 1, -z + 1$.]

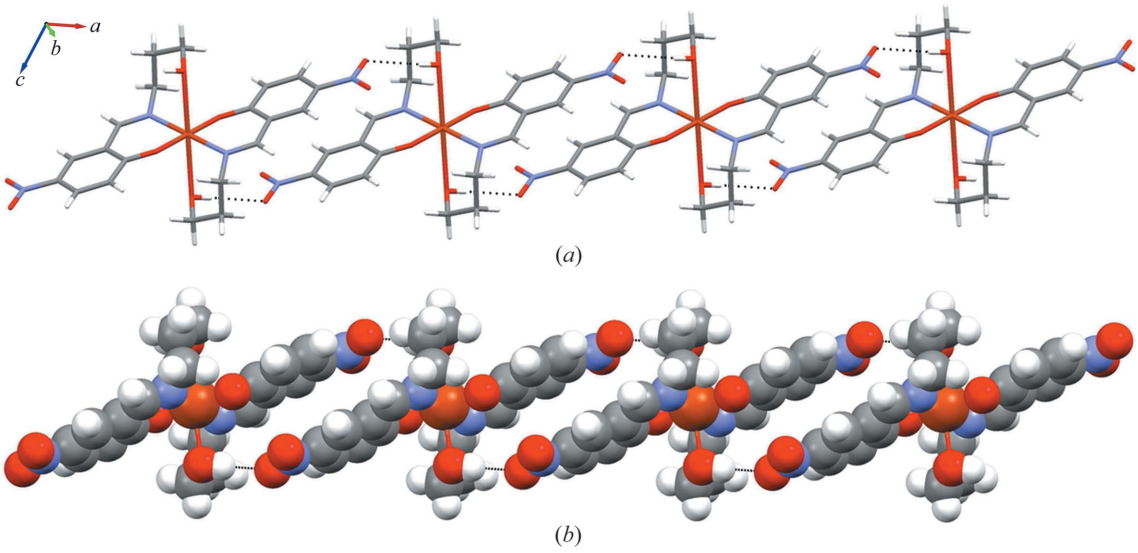

Figure 2
(*a*) A perspective view of the one-dimensional chain structure of (1) along the [100] direction, showing the intermolecular O—H···O hydrogen bonds (dashed lines). (*b*) A space-filling representation of complex (1).

Table 2
Selected geometric parameters (Å, °).

Cu1—O1	2.648 (4)	Cu1—N1	2.008 (3)
Cu1—O2	1.931 (3)		
O2—Cu1—O1	94.75 (11)	O2—Cu1—N1	90.03 (12)
O2—Cu1—O1^{i}	85.25 (11)	N1—Cu1—O1	76.37 (12)
O2—Cu1—N1^{i}	89.97 (12)	N1—Cu1—O1^{i}	103.63 (12)

Symmetry code: (i) $-x, -y+1, -z+1$.

monohydrate (1 mmol) in hot methanol (30 ml) to a solution of H_2L (1 mmol) in hot methanol (30 ml). The combined solution was warmed to 338 K and stirred for 1 h. The resulting solution was filtered rapidly and allowed to stand at room temperature. After several weeks, green crystals (yield 75%) of complex (1) suitable for X-ray analysis were obtained. The synthetic route is outlined in Scheme 1. Analysis calculated for $C_{20}H_{22}CuN_4O_8$: C 47.10, H 4.35, N 10.99%; found: C 47.11, H 4.37, N 10.98%.

2.2. Refinement

Crystal data, data collection and structure refinement details are summarized in Table 1. H-atom positions were calculated geometrically and refined using the riding model.

3. Results and discussion

3.1. Crystal structure

The title complex, (1) (Fig. 1), crystallizes in the monoclinic space group $P2_1/c$ and its asymmetric unit consists of half of a $[Cu(HL)_2]$ unit. The Cu^{II} atom lies on a centre of inversion, and is coordinated by two deprotonated tridentate Schiff base ligands (*HL*) through two imine N atoms, two phenoxy O atoms in a mutual *trans* disposition and two alkoxy O atoms in axial positions. The geometry of the Cu^{II} atom is best described as an elongated octahedral coordination with Jahn–Teller distortion. Selected bond lengths and angles are listed in Table 2 and lie well within the ranges reported for corresponding bond lengths and angles in other mononuclear copper(II) complexes (Fernández-G. *et al.*, 2006; Mitra *et al.*, 2013; Li *et al.*, 2012).

In the crystalline architecture of (1), the aliphatic –OH group of the Schiff base ligand actively participates in intermolecular O—H···O hydrogen bonds connecting one other unit and thus stabilizing the crystal lattice (Table 3). This results in a one-dimensional chain structure along the [100] direction. The intermolecular Cu···Cu^{ii} [symmetry code: (ii) $-x+1, -y+1, -z+1$] distance is 10.579 (5) Å in this chain structure (Fig. 2). Intermolecular π–π contacts also connect the molecules into a three-dimensional structure (Fig. 3 and

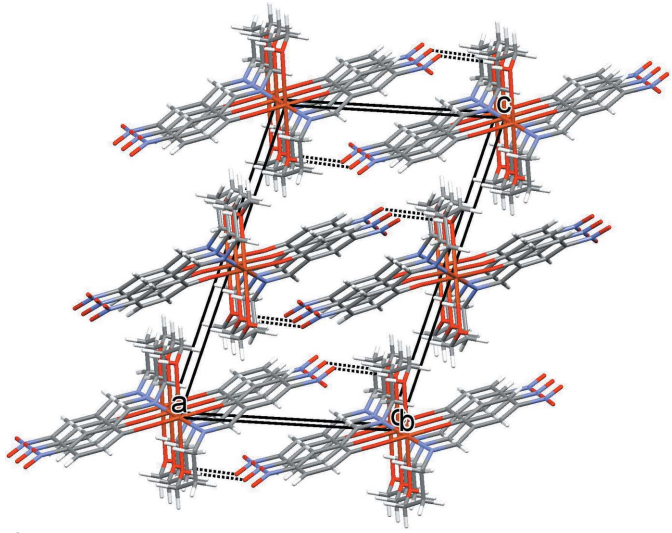

Figure 3
(*a*) A view of the crystal packing of the polymeric networks projected along the [010] direction and the stacks along the [010] direction, showing the intermolecular O—H···O hydrogen bonds (dashed lines).

Table 3
Short-contact and hydrogen-bond geometry (Å, °) for complex (1).

CgI is the plane number *I*, *CgI*···*CgJ* is the distance between ring centroids, *CgI*_Perp is the perpendicular distance of *CgI* on ring *J*, *CgJ*_Perp is the perpendicular distance of *CgJ* on ring *I* and *Cg*1 is the centroid of the C5–C10 ring.

CgI···*CgJ*	*CgI*···*CgJ*	*CgI*_Perp	*CgJ*_Perp	
*Cg*1···*Cg*1^{ii}	3.801 (3)	3.4584 (18)	3.4584 (19)	
D—H···*A*	*D*—H	H···*A*	*D*···*A*	*D*—H···*A*
O1—H1···O4^{ii}	0.82	2.24	3.023 (4)	160

Symmetry code: (ii) $-x+1, -y+1, -z+1$.

Table 3). This hydrogen-bonded polymeric network lies in the *ac* plane and stacks along the *b* axis (Fig. 3).

3.2. IR spectra

The IR spectrum of complex (1) (see Fig. S1 in the *Supporting information*) was analysed in comparison with that of free H_2L in the range 4000–600 cm^{-1}; the characteristic IR frequencies are summarized in Table 4. The IR spectrum of free H_2L shows a broad band in the region of 3274 cm^{-1} attributed to ν(O—H) stretching, which disappears in complex (1), indicating deprotonation of the phenolic hydroxy group upon complexation (Gungor & Kara, 2011). Several weak peaks in the range 2955–2841 cm^{-1} are likely to be due to the characteristic aromatic and aliphatic ν(C—H) vibrations for the ligand and complex (1) (Gungor & Kara, 2015). The IR spectrum of free H_2L show a strong absorption band at 1660 cm^{-1}, which is attributed to characteristic ν(C═N) stretching. This band is shifted to a lower frequency (~1626 cm^{-1}) for complex (1), which suggests coordination between the imine N atoms and the Cu^{II} atom (Yahsi *et al.*, 2016). Symmetric and asymmetric ν(C—NO$_2$) stretches were observed in the range 1523–1349 cm^{-1} for free H_2L and complex (1). The IR spectra show weak bands in the range 1241–1213 cm^{-1} which were assigned to ν(C—N) (Hopa & Cokay, 2016*a*,*b*; Olalekan *et al.*, 2016). Thus, the IR spectra are found to be in good agreement with the structural features of complex (1).

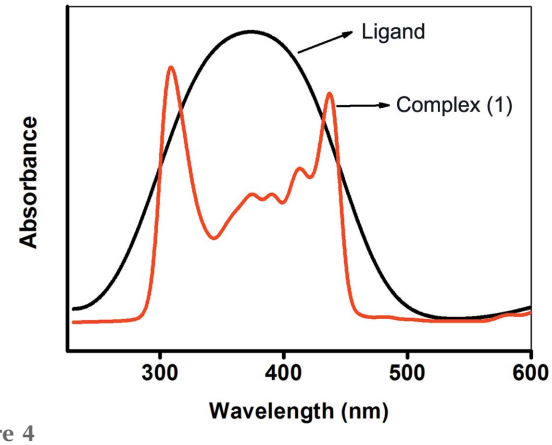

Figure 4
The solid-state UV–Vis spectra of free H_2L and complex (1).

Table 4
The IR spectroscopic details for complex (1) and H_2L (cm^{-1}).

	ν(O—H)	ν(C—H)	ν(C═N)	ν(C═C)	ν(C—O)	ν(C—NO$_2$)
H_2L	3274, 3510	2922–2841	1660	1603	1322, 1285	1523, 1371
(1)	3549	2955–2877	1626	1594	1300	1481, 1349

3.3. Solid-state UV–Vis spectra

A comparison of the solid-state UV–Vis spectra of free H_2L and complex (1) is shown in Fig. 4. The electronic spectrum of free H_2L shows a high absorption band at 373 nm, which may arise because of the conjugated system. On complexation, the broad absorption band is divided into two sharp absorption bands; one of these bands is shifted to lower energy at 437 nm and the other is shifted to higher energy at 309 nm compared to free H_2L. The maximum observed at 437 nm is related to π–π* transitions of the imine groups. In addition, the maximum at 309 nm is related to n–π* transitions of the phenyl rings (Lever, 1984). It was not possible to identify *d*–*d* transitions due to a strong charge-transfer band tailing from the UV to the visible region (Emara & Adly, 2007; Emara *et al.*, 2008).

3.4. Photoluminescence properties

The solid-state photoluminescence properties of complex (1) and free H_2L were investigated at room temperature in the visible region upon excitation at λ_{ex}= 349 nm (Fig. 5). Free H_2L displays a broad emission band at λ_{max} = 480 nm which may be assigned to the $n\rightarrow\pi^*$ or $\pi\rightarrow\pi^*$ electronic transitions (ILCT) (Feng *et al.*, 2014; Hopa & Cokay, 2016*a*,*b*). When H_2L is combined with Cu^{II} in complex (1), an intense green emission band is seen at λ_{max} = 520 nm. The observed red shift of the emission maximum between complex (1) and free H_2L was considered to originate mainly from the influence of the coordination of the metal atom to H*L* (Wu *et al.*, 2006; Manjunatha *et al.*, 2011). Moreover, the enhancement of the luminescence intensity of complex (1) compared to free H_2L is

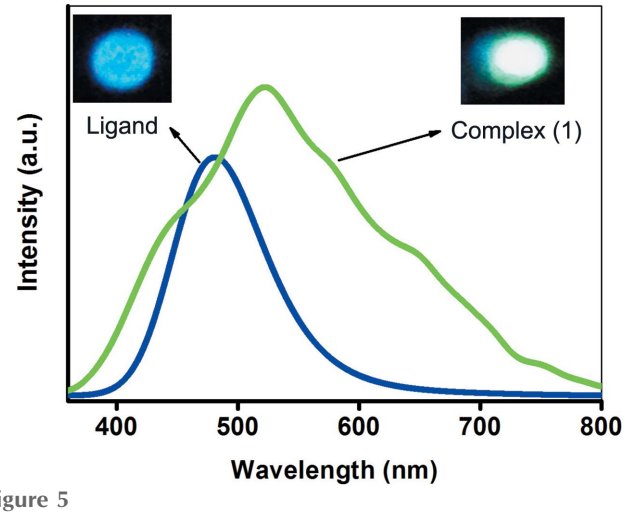

Figure 5
The emission spectra of free H_2L and complex (1) in solid samples at room temperature (λ_{ex} = 349 nm).

due to the fact that formation of the metal complex effectively increases the 'rigidity' of the ligand and thus reduces the loss of energy *via* radiationless thermal vibrations (Chen *et al.*, 2011; Ji *et al.*, 2012; Zheng *et al.*, 2001; Wang *et al.*, 2006; Gao *et al.*, 2015).

4. Conclusions

A new monomeric Cu^{II}–Schiff base complex, (1), has been synthesized and characterized by elemental analysis, UV–Vis and IR spectroscopies, single-crystal X-ray diffraction analysis and a photoluminescence study. The crystal structure analysis of (1) shows that the Cu^{II} atom lies on a centre of inversion, and is coordinated by two tridentate Schiff base ligands (H_2L) using ONO donors. Intermolecular O—H···O hydrogen bonds link the molecules into one-dimensional chains along the [100] direction and π–π contacts connect the molecules into a three-dimensional structure. Furthermore, photoluminescence studies of complex (1) show a red shift and a stronger emission compared with free H_2L as a result of the influence of the coordination of the metal atom to the ligand. The luminescence properties show that the photoluminescence arose from intraligand emission and that the title complex is a novel potential candidate for application in optoelectronic devices.

Acknowledgements

The authors are grateful to the Research Funds of Mugla Sitki Kocman University (BAP-2016/052) for financial support and to Dokuz Eylül University for the use of the Agilent Xcalibur Eos diffractometer (purchased under University Research grant No. 2010.KB.FEN.13). The authors also acknowledge Balikesir University, Science and Technology Application and Research Center (BUBTAM), for the use of the photoluminescence spectrometer.

References

Blacque, O., Amjad, A., Caneschi, A., Sorace, L. & Car, P.-E. (2016). *New J. Chem.* **40**, 3571–3577.
Caneschi, A., Gatteschi, D. & Totti, F. (2015). *Coord. Chem. Rev.* **289–290**, 357–378.
Celen, S., Gungor, E., Kara, H. & Azaz, A. D. (2013). *J. Coord. Chem.* **66**, 3170–3181.
Chang, M., Chung, M., Lee, B. S. & Kwak, C. (2006). *J. Nanosci. Nanotechnol.* **6**, 3338–3342.
Chen, Y. N., Ge, Y. Y., Zhou, W., Ye, L. F., Gu, Z. G., Ma, G. Z., Li, W. S., Li, H. & Cai, Y. P. (2011). *Inorg. Chem. Commun.* **14**, 1228–1232.
Clark, R. C. & Reid, J. S. (1995). *Acta Cryst.* A**51**, 887–897.
Delgado, S., Santana, A., Castillo, O. & Zamora, F. (2010). *Dalton Trans.* **39**, 2280–2287.
Dolomanov, O. V., Bourhis, L. J., Gildea, R. J., Howard, J. A. K. & Puschmann, H. (2009). *J. Appl. Cryst.* **42**, 339–341.
Emara, A. A. A. & Adly, O. M. I. (2007). *Transition Met. Chem.* **32**, 889–901.
Emara, A. A. A., El-Sayed, B. A. & Ahmed, E.-S. A. E. (2008). *Spectrochim. Acta Part A*, **69**, 757–769.
Erkarslan, U., Oylumluoglu, G., Coban, M. B., Öztürk, E. & Kara, H. (2016). *Inorg. Chim. Acta*, **445**, 57–61.
Feng, X., Feng, Y.-Q., Chen, J. J., Ng, S.-W., Wang, L.-Y. & Guo, J.-Z. (2014). *Dalton Trans.* **44**, 804–816.
Fernández-G., J. M., Tepal-Sánchez, P. & Hernández-Ortega, S. (2006). *J. Mol. Struct.* **787**, 1–7.
Freitag, M., Giordano, F., Yang, W., Pazoki, M., Hao, Y., Zietz, B., Grätzel, M., Hagfeldt, A. & Boschloo, G. (2016). *J. Phys. Chem. C*, **120**, 9595–9603.
Gao, Q., Qin, Y., Chen, Y., Liu, W., Li, H., Wu, B., Li, Y. & Li, W. (2015). *RSC Adv.* **5**, 43195–43201.
Gungor, E. (2017). *Mol. Cryst. Liq. Cryst.* **642**, 21–28.
Gungor, E., Celen, S., Azaz, D. & Kara, H. (2012). *Spectrochim. Acta Part A*, **94**, 216–221.
Gungor, E. & Kara, H. (2011). *Spectrochim. Acta Part A*, **82**, 217–220.
Gungor, E. & Kara, H. (2012). *Inorg. Chim. Acta*, **384**, 137–142.
Gungor, E. & Kara, H. (2015). *J. Struct. Chem.* **56**, 1646–1652.
Gungor, E., Kara, H., Colacio, E. & Mota, A. J. (2014). *Eur. J. Inorg. Chem.* pp. 1552–1560.
Gungor, E., Yahsi, Y., Kara, H. & Caneschi, A. (2015). *CrystEngComm*, **17**, 3082–3088.
Hopa, C. & Cokay, I. (2016*a*). *Acta Cryst.* C**72**, 601–606.
Hopa, C. & Cokay, I. (2016*b*). *Acta Cryst.* C**72**, 149–154.
Jamaludin, N. S., Abdul Halim, S. N., Khoo, C.-H., Chen, B.-J., See, T.-H., Sim, J.-H., Cheah, Y.-K., Seng, H.-L. & Tiekink, E. R. T. (2016). *Z. Kristallogr. Cryst. Mater.* **231**, 341–349.
Ji, Y.-F., Wang, R., Ding, S., Du, C.-F. & Liu, Z.-L. (2012). *Inorg. Chem. Commun.* **16**, 47–50.
Kahn, O. (1993). In *Molecular Magnetism*. New York: VCH.
Karakas, A., Elmali, A., Unver, H., Kara, H. & Yahsi, Y. (2006). *Z. Naturforsch. Teil B*, **61**, 968–974.
Kelley, T. W., Baude, P. F., Gerlach, C., Ender, D. E., Muyres, D., Haase, M. A., Vogel, D. E. & Theiss, S. D. (2004). *Chem. Mater.* **16**, 4413–4422.
Keypour, H., Shayesteh, M., Rezaeivala, M. & Sayin, K. (2016). *J. Mol. Struct.* **1112**, 110–118.
Keypour, H., Zeynali, H., Rezaeivala, M., Mohsenzadeh, F., Rudbari, H. A., Bruno, G. & Sadeghpour, A. (2015). *J. Iran. Chem. Soc.* **12**, 1665–1675.
Kongchoo, S., Kantacha, A., Saithong, S. & Wongnawa, S. (2016). *J. Chem. Crystallogr.* **46**, 222–229.
Lever, A. B. P. (1984). In *Inorganic Electronic Spectroscopy*. Amsterdam: Elsevier.
Li, Y., Li, Z., Liu, Y., Dong, X. & Cui, Y. (2012). *J. Coord. Chem.* **65**, 19–27.
Li, L.-L., Liu, L.-L., Ren, Z.-G., Li, H.-X., Zhang, Y. & Lang, J.-P. (2009). *CrystEngComm*, **11**, 2751–2756.
Magni, M., Giannuzzi, R., Colombo, A., Cipolla, M. P., Dragonetti, C., Caramori, S., Carli, S., Grisorio, R., Suranna, G. P., Bignozzi, C. A., Roberto, D. & Manca, M. (2016). *Inorg. Chem.* **55**, 5245–5253.
Manjunatha, M. N., Dikundwar, A. G. & Nagasundara, K. R. (2011). *Polyhedron*, **30**, 1299–1304.
Mitra, M., Maji, A. K., Ghosh, B. K., Kaur, G., Roy Choudhury, A., Lin, C.-H., Ribas, J. & Ghosh, R. (2013). *Polyhedron*, **61**, 15–19.
Naskar, S., Naskar, S., Butcher, R. J. & Chattopadhyay, S. K. (2010). *Inorg. Chim. Acta*, **363**, 404–411.
Obali, A. Y. & Ucan, H. I. (2015). *J. Mol. Struct.* **1081**, 74–78.
Olalekan, T. E., Ogunlaja, A. S., VanBrecht, B. & Watkins, G. M. (2016). *J. Mol. Struct.* **1122**, 72–79.
Pal, T. K., De, D., Senthilkumar, S., Neogi, S. & Bharadwaj, P. K. (2016). *Inorg. Chem.* **55**, 7835–7842.
Paul, A., Ribeiro, A. P. C., Karmakar, A., Guedes da Silva, M. F. C. & Pombeiro, A. J. L. (2016). *Dalton Trans.* **45**, 12779–12789.
Petrova, P. & Tomova, R. (2009). *Bulg. Chem. Commun.* **41**, 211–225.
Rigaku OD (2015). *CrysAlis PRO*. Rigaku Oxford Diffraction Ltd, Yarnton, Oxfordshire, England.
Safaei, E., Kabir, M. M., Wojtczak, A., Jagličić, Z., Kozakiewicz, A. & Lee, Y.-I. (2011). *Inorg. Chim. Acta*, **366**, 275–282.

Sasabe, H. & Kido, J. (2011). *Chem. Mater.* **23**, 621–630.
Sheldrick, G. M. (2015*a*). *Acta Cryst.* A**71**, 3–8.
Sheldrick, G. M. (2015*b*). *Acta Cryst.* C**71**, 3–8.
Wang, Y., Yi, L., Yang, X., Ding, B., Cheng, P., Liao, D.-Z. & Yan, S.-P. (2006). *Inorg. Chem.* **45**, 5822–5829.
Wu, G., Wang, X.-F., Okamura, T., Sun, W.-Y. & Ueyama, N. (2006). *Inorg. Chem.* **45**, 8523–8532.
Wu, W., Xie, J. & Xie, D. (2010). *Russ. J. Inorg. Chem.* **55**, 384–389.
Yahsi, Y. (2016). *Acta Cryst.* C**72**, 585–592.
Yahsi, Y. & Kara, H. (2013). *Inorg. Chim. Acta*, **397**, 110–116.
Yahsi, Y., Ozbek, H., Aygun, M. & Kara, H. (2016). *Acta Cryst.* C**72**, 426–431.
Zheng, S.-L., Tong, M.-L., Tan, S.-D., Wang, Y., Shi, J.-X., Tong, Y.-X., Lee, H. K. & Chen, X.-M. (2001). *Organometallics*, **20**, 5319–5325.
Zheng, S.-R., Zhang, L., He, J.-E., Fan, J. & Zhang, W.-G. (2016). *Inorg. Chem. Commun.* **66**, 19–23.
Zhou, X., Yu, B., Guo, Y., Tang, X., Zhang, H. & Liu, W. (2010). *Inorg. Chem.* **49**, 4002–4007.

supporting information

Acta Cryst. (2017). C**73**, 414-419 [https://doi.org/10.1107/S2053229617005976]

Crystal structure and photoluminescence properties of a new monomeric copper(II) complex: bis(3-{[(3-hydroxypropyl)imino]methyl}-4-nitrophenolato-κ^3O,N,O')copper(II)

Cagdas Kocak, Gorkem Oylumluoglu, Adem Donmez, M. Burak Coban, Ugur Erkarslan, Muhittin Aygun and Hulya Kara

Computing details

Data collection: *CrysAlis PRO* (Rigaku OD, 2015); cell refinement: *CrysAlis PRO* (Rigaku OD, 2015); data reduction: *CrysAlis PRO* (Rigaku OD, 2015); program(s) used to solve structure: SHELXT (Sheldrick, 2015a); program(s) used to refine structure: *SHELXL2016* (Sheldrick, 2015b); molecular graphics: OLEX2 (Dolomanov *et al.*, 2009); software used to prepare material for publication: OLEX2 (Dolomanov *et al.*, 2009).

Bis(3-{[(3-hydroxypropyl)imino]methyl}-4-nitrophenolato-κ^3O,N,O')copper(II)

Crystal data

$[Cu(C_{10}H_{11}N_2O_4)_2]$
M_r = 509.95
Monoclinic, $P2_1/c$
a = 10.5788 (11) Å
b = 6.2806 (5) Å
c = 15.8478 (19) Å
β = 105.272 (12)°
V = 1015.76 (19) Å^3
Z = 2
$F(000)$ = 526
D_x = 1.667 Mg m^{-3}
Mo $K\alpha$ radiation, λ = 0.71073 Å
Cell parameters from 812 reflections
θ = 3.7–22.9°
μ = 1.14 mm^{-1}
T = 292 K
Plate, green
0.25 × 0.15 × 0.06 mm

Data collection

Rigaku OD Xcalibur Eos diffractometer
Detector resolution: 8.0667 pixels mm^{-1}
ω scans
Absorption correction: analytical [CrysAlis PRO (Rigaku OD, 2015) based on expressions derived by Clark & Reid (1995)]
T_{min} = 0.823, T_{max} = 0.947
3722 measured reflections
1908 independent reflections
1303 reflections with $I > 2\sigma(I)$
R_{int} = 0.046
θ_{max} = 25.7°, θ_{min} = 3.5°
h = −12→9
k = −7→5
l = −18→19

Refinement

Refinement on F^2
Least-squares matrix: full
$R[F^2 > 2\sigma(F^2)]$ = 0.056
$wR(F^2)$ = 0.120
S = 1.03
1908 reflections
152 parameters
0 restraints
Primary atom site location: structure-invariant direct methods
Hydrogen site location: inferred from neighbouring sites
H-atom parameters constrained

$w = 1/[\sigma^2(F_o^2) + (0.0404P)^2]$
where $P = (F_o^2 + 2F_c^2)/3$
$(\Delta/\sigma)_{max} < 0.001$

$\Delta\rho_{max} = 0.46$ e Å^{-3}
$\Delta\rho_{min} = -0.44$ e Å^{-3}

Special details

Geometry. All e.s.d.'s (except the e.s.d. in the dihedral angle between two l.s. planes) are estimated using the full covariance matrix. The cell e.s.d.'s are taken into account individually in the estimation of e.s.d.'s in distances, angles and torsion angles; correlations between e.s.d.'s in cell parameters are only used when they are defined by crystal symmetry. An approximate (isotropic) treatment of cell e.s.d.'s is used for estimating e.s.d.'s involving l.s. planes.

Fractional atomic coordinates and isotropic or equivalent isotropic displacement parameters (Å²)

	x	*y*	*z*	U_{iso}*/U_{eq}
Cu1	0.000000	0.500000	0.500000	0.0286 (3)
O1	0.0989 (3)	0.4425 (5)	0.6702 (2)	0.0460 (9)
H1	0.176143	0.416414	0.674076	0.069*
O2	0.1378 (3)	0.3461 (4)	0.4671 (2)	0.0330 (8)
O3	0.5874 (3)	0.8420 (6)	0.3669 (2)	0.0552 (11)
O4	0.6111 (3)	0.5323 (5)	0.3162 (2)	0.0539 (10)
N1	0.1206 (3)	0.7498 (5)	0.5363 (2)	0.0248 (8)
N2	0.5543 (4)	0.6560 (6)	0.3538 (3)	0.0365 (10)
C1	0.0895 (5)	0.6305 (7)	0.7191 (3)	0.0414 (13)
H1A	0.127875	0.601452	0.780692	0.050*
H1B	−0.002340	0.663412	0.711707	0.050*
C2	0.1560 (4)	0.8230 (7)	0.6936 (3)	0.0359 (12)
H2A	0.247528	0.788726	0.700176	0.043*
H2B	0.152832	0.937389	0.734064	0.043*
C3	0.0980 (4)	0.9032 (6)	0.6012 (3)	0.0312 (11)
H3A	0.004588	0.925461	0.591842	0.037*
H3B	0.137556	1.038768	0.593663	0.037*
C4	0.2233 (4)	0.7797 (7)	0.5107 (3)	0.0268 (10)
H4	0.268637	0.905676	0.528558	0.032*
C5	0.2773 (4)	0.6396 (6)	0.4570 (3)	0.0245 (10)
C6	0.3836 (4)	0.7086 (7)	0.4286 (3)	0.0286 (11)
H6	0.414578	0.846620	0.441353	0.034*
C7	0.4442 (4)	0.5766 (7)	0.3818 (3)	0.0295 (11)
C8	0.4019 (4)	0.3672 (7)	0.3639 (3)	0.0328 (11)
H8	0.443455	0.277462	0.332954	0.039*
C9	0.2984 (4)	0.2962 (7)	0.3925 (3)	0.0309 (11)
H9	0.269857	0.156892	0.379817	0.037*
C10	0.2332 (4)	0.4250 (6)	0.4404 (3)	0.0256 (10)

Atomic displacement parameters (Å²)

	U^{11}	U^{22}	U^{33}	U^{12}	U^{13}	U^{23}
Cu1	0.0254 (4)	0.0264 (4)	0.0368 (5)	−0.0030 (4)	0.0132 (4)	−0.0020 (4)
O1	0.047 (2)	0.0414 (19)	0.052 (2)	0.0018 (18)	0.016 (2)	0.0030 (17)
O2	0.0263 (17)	0.0268 (16)	0.049 (2)	−0.0049 (15)	0.0164 (16)	−0.0047 (15)
O3	0.049 (2)	0.056 (2)	0.070 (3)	−0.020 (2)	0.032 (2)	−0.001 (2)

O4	0.040 (2)	0.065 (2)	0.067 (3)	0.004 (2)	0.032 (2)	0.002 (2)
N1	0.0221 (19)	0.0233 (18)	0.031 (2)	0.0027 (18)	0.0097 (17)	−0.0012 (17)
N2	0.026 (2)	0.048 (3)	0.038 (2)	0.002 (2)	0.013 (2)	0.007 (2)
C1	0.045 (3)	0.047 (3)	0.035 (3)	0.006 (3)	0.015 (3)	0.002 (2)
C2	0.034 (3)	0.039 (3)	0.036 (3)	0.003 (2)	0.010 (2)	−0.018 (2)
C3	0.032 (3)	0.025 (2)	0.041 (3)	−0.006 (2)	0.017 (2)	−0.011 (2)
C4	0.026 (2)	0.025 (2)	0.028 (3)	−0.006 (2)	0.004 (2)	0.000 (2)
C5	0.023 (2)	0.026 (2)	0.024 (2)	0.002 (2)	0.007 (2)	−0.003 (2)
C6	0.026 (2)	0.028 (2)	0.031 (3)	−0.002 (2)	0.005 (2)	0.003 (2)
C7	0.020 (2)	0.039 (3)	0.030 (3)	0.000 (2)	0.008 (2)	0.004 (2)
C8	0.029 (3)	0.040 (3)	0.031 (3)	0.009 (2)	0.010 (2)	−0.002 (2)
C9	0.031 (3)	0.024 (2)	0.037 (3)	−0.003 (2)	0.009 (2)	−0.004 (2)
C10	0.018 (2)	0.028 (2)	0.027 (2)	0.002 (2)	0.000 (2)	0.002 (2)

Geometric parameters (Å, º)

Cu1—O1^{i}	2.648 (4)	C2—H2A	0.9700
Cu1—O1	2.648 (4)	C2—H2B	0.9700
Cu1—O2	1.931 (3)	C2—C3	1.516 (6)
Cu1—O2^{i}	1.931 (3)	C3—H3A	0.9700
Cu1—N1	2.008 (3)	C3—H3B	0.9700
Cu1—N1^{i}	2.008 (3)	C4—H4	0.9300
O1—H1	0.8200	C4—C5	1.443 (5)
O1—C1	1.431 (5)	C5—C6	1.386 (6)
O2—C10	1.292 (5)	C5—C10	1.428 (6)
O3—N2	1.221 (4)	C6—H6	0.9300
O4—N2	1.228 (4)	C6—C7	1.378 (5)
N1—C3	1.474 (5)	C7—C8	1.394 (6)
N1—C4	1.269 (5)	C8—H8	0.9300
N2—C7	1.441 (5)	C8—C9	1.365 (6)
C1—H1A	0.9700	C9—H9	0.9300
C1—H1B	0.9700	C9—C10	1.409 (5)
C1—C2	1.507 (6)		

O1—Cu1—O1^{i}	180.0	C1—C2—H2B	108.5
O2^{i}—Cu1—O1^{i}	94.75 (11)	C1—C2—C3	115.3 (4)
O2—Cu1—O1	94.75 (11)	H2A—C2—H2B	107.5
O2—Cu1—O1^{i}	85.25 (11)	C3—C2—H2A	108.5
O2^{i}—Cu1—O1	85.25 (11)	C3—C2—H2B	108.5
O2—Cu1—O2^{i}	180.00 (9)	N1—C3—C2	111.0 (3)
O2—Cu1—N1^{i}	89.97 (12)	N1—C3—H3A	109.4
O2^{i}—Cu1—N1^{i}	90.03 (12)	N1—C3—H3B	109.4
O2^{i}—Cu1—N1	89.97 (12)	C2—C3—H3A	109.4
O2—Cu1—N1	90.03 (12)	C2—C3—H3B	109.4
N1^{i}—Cu1—O1^{i}	76.37 (12)	H3A—C3—H3B	108.0
N1—Cu1—O1	76.37 (12)	N1—C4—H4	116.4
N1—Cu1—O1^{i}	103.63 (12)	N1—C4—C5	127.1 (4)
N1^{i}—Cu1—O1	103.63 (12)	C5—C4—H4	116.4

N1^{i}—Cu1—N1	180.0	C6—C5—C4	118.8 (4)
Cu1—O1—H1	102.9	C6—C5—C10	119.3 (4)
C1—O1—Cu1	112.0 (3)	C10—C5—C4	121.6 (4)
C1—O1—H1	109.5	C5—C6—H6	119.4
C10—O2—Cu1	127.4 (3)	C7—C6—C5	121.2 (4)
C3—N1—Cu1	120.2 (3)	C7—C6—H6	119.4
C4—N1—Cu1	123.8 (3)	C6—C7—N2	119.1 (4)
C4—N1—C3	115.8 (4)	C6—C7—C8	120.5 (4)
O3—N2—O4	122.2 (4)	C8—C7—N2	120.4 (4)
O3—N2—C7	119.8 (4)	C7—C8—H8	120.6
O4—N2—C7	118.0 (4)	C9—C8—C7	118.9 (4)
O1—C1—H1A	108.7	C9—C8—H8	120.6
O1—C1—H1B	108.7	C8—C9—H9	118.6
O1—C1—C2	114.4 (4)	C8—C9—C10	122.7 (4)
H1A—C1—H1B	107.6	C10—C9—H9	118.6
C2—C1—H1A	108.7	O2—C10—C5	123.2 (4)
C2—C1—H1B	108.7	O2—C10—C9	119.5 (4)
C1—C2—H2A	108.5	C9—C10—C5	117.3 (4)
Cu1—O1—C1—C2	−57.7 (5)	C3—N1—C4—C5	171.3 (4)
Cu1—O2—C10—C5	21.1 (6)	C4—N1—C3—C2	−92.6 (4)
Cu1—O2—C10—C9	−159.0 (3)	C4—C5—C6—C7	175.9 (4)
Cu1—N1—C3—C2	83.0 (4)	C4—C5—C10—O2	4.4 (6)
Cu1—N1—C4—C5	−4.1 (6)	C4—C5—C10—C9	−175.5 (4)
O1—C1—C2—C3	64.3 (5)	C5—C6—C7—N2	180.0 (4)
O3—N2—C7—C6	−4.5 (6)	C5—C6—C7—C8	−1.7 (7)
O3—N2—C7—C8	177.3 (4)	C6—C5—C10—O2	177.7 (4)
O4—N2—C7—C6	176.2 (4)	C6—C5—C10—C9	−2.3 (6)
O4—N2—C7—C8	−2.0 (6)	C6—C7—C8—C9	0.8 (7)
N1—C4—C5—C6	173.8 (4)	C7—C8—C9—C10	−0.7 (7)
N1—C4—C5—C10	−12.9 (7)	C8—C9—C10—O2	−178.5 (4)
N2—C7—C8—C9	179.1 (4)	C8—C9—C10—C5	1.4 (6)
C1—C2—C3—N1	−68.0 (5)	C10—C5—C6—C7	2.5 (6)

Symmetry code: (i) −*x*, −*y*+1, −*z*+1.

Hydrogen-bond geometry (Å, º)

D—H···*A*	*D*—H	H···*A*	*D*···*A*	*D*—H···*A*
O1—H1···O4^{ii}	0.82	2.24	3.023 (4)	160

Symmetry code: (ii) −*x*+1, −*y*+1, −*z*+1.